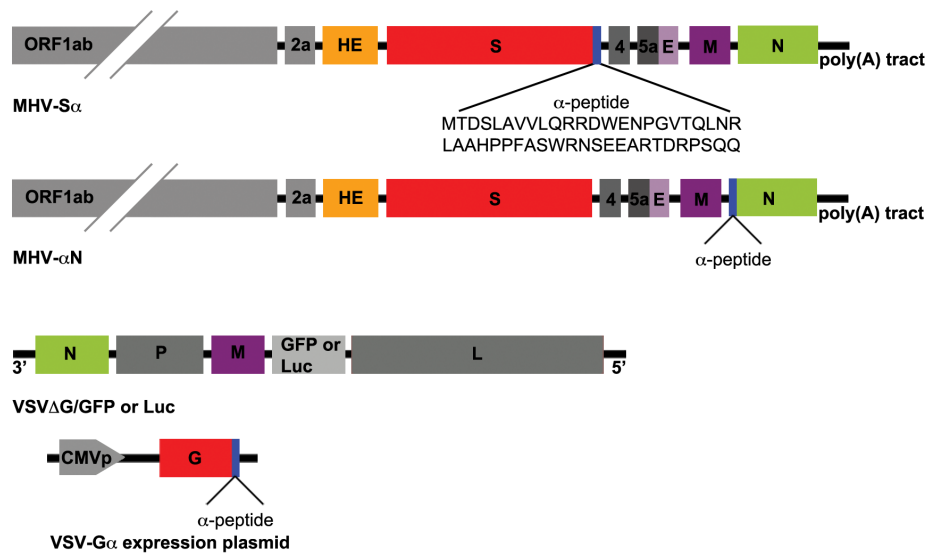
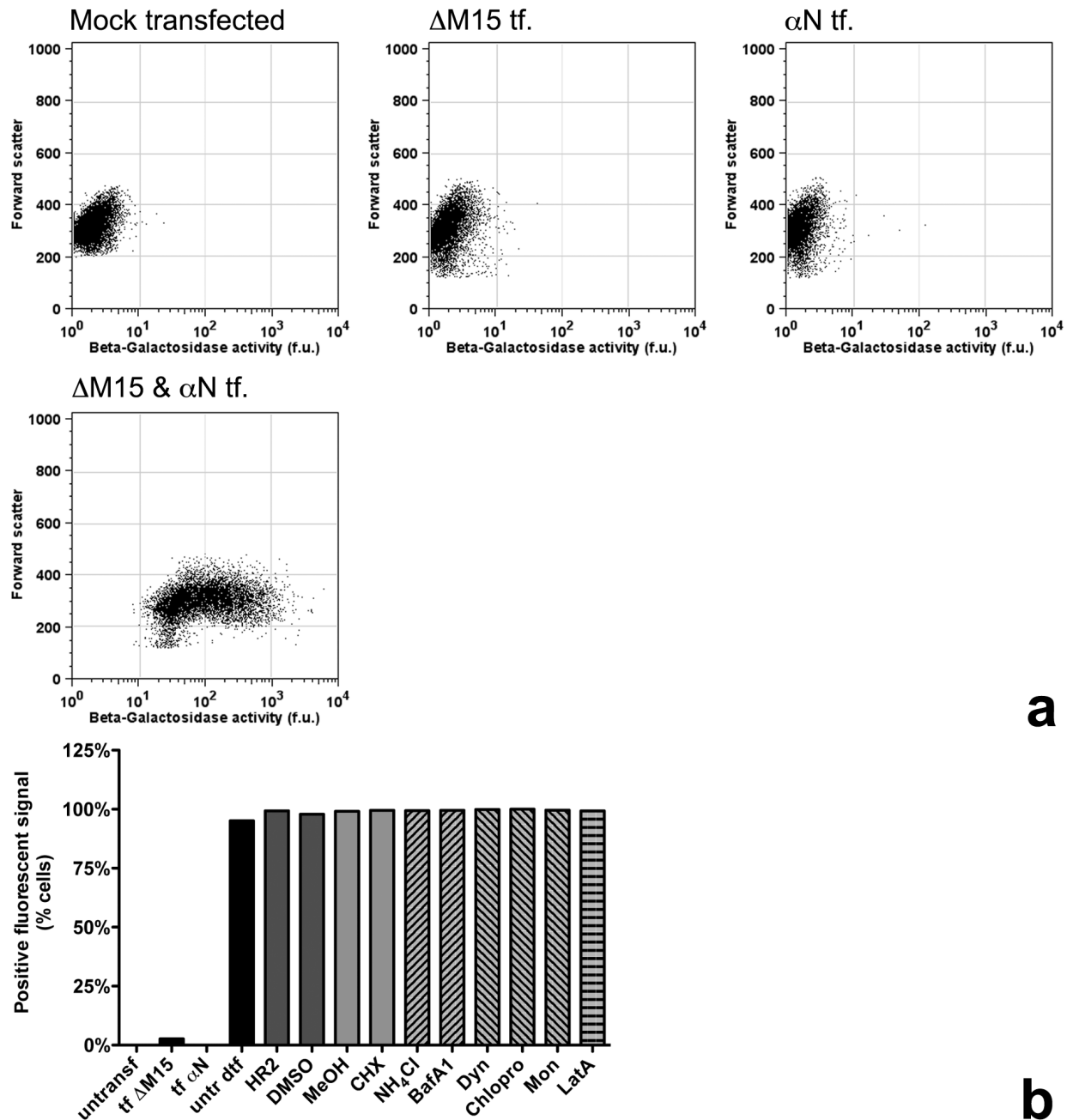


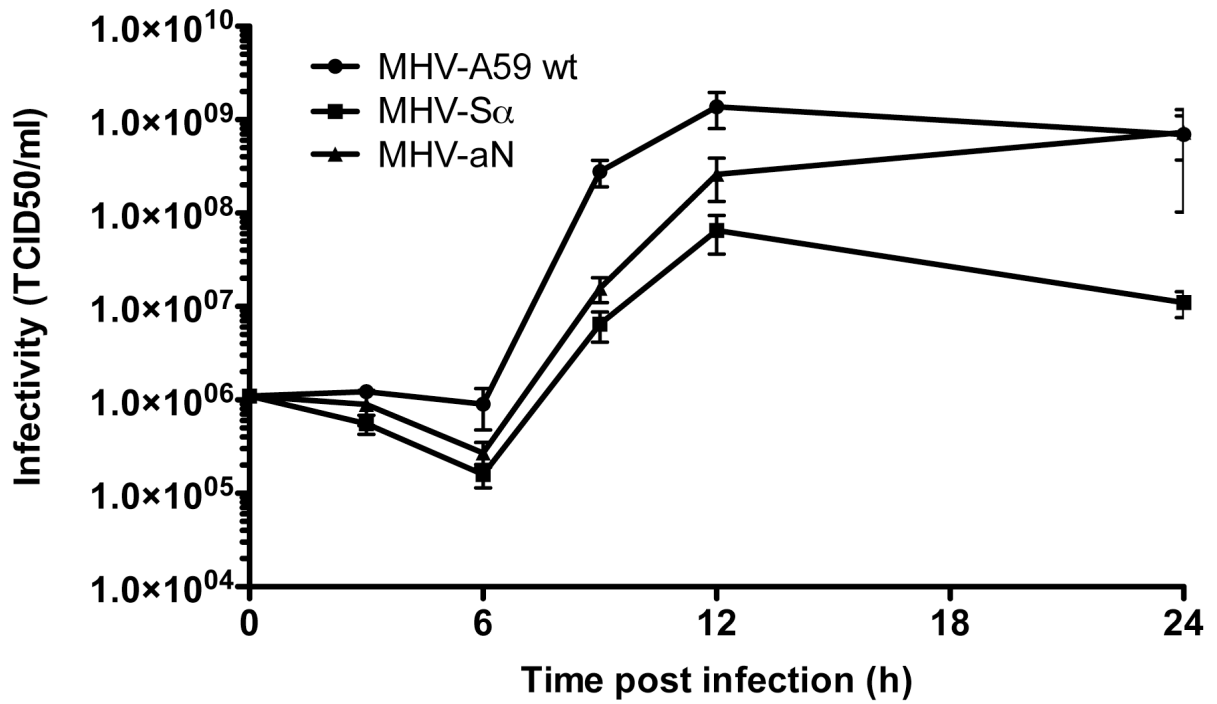
## SUPPLEMENTARY INFORMATION



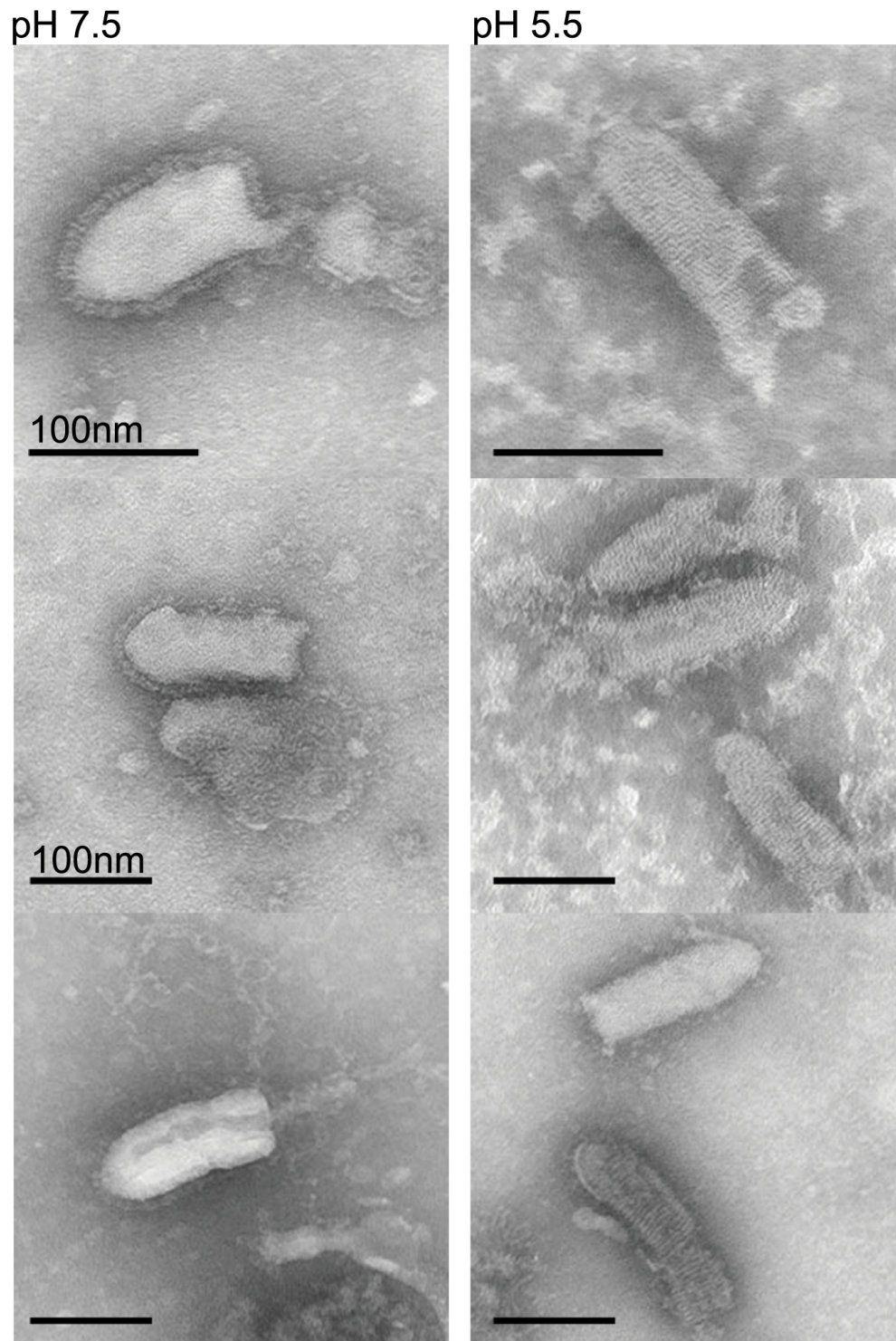
- 1 **Figure S1.** Schematic layout of the genome of recombinant viruses. MHV-S $\alpha$ , encoding C-
- 2 terminally  $\alpha$ -peptide-tagged spike protein (top). MHV- $\alpha$ N, encoding the N-terminally  $\alpha$ -
- 3 peptide-tagged nucleocapsid protein (middle) and pseudotyped VSV $\Delta$ G/GFP or -Luc virus
- 4 coding a GFP or firefly luciferase expression cassette substituting the gene encoding the G
- 5 protein. C-terminally tagged VSV-G $\alpha$  is provided by the producer cells stably expressing VSV-
- 6 G $\alpha$  under the control of a CMV promoter.



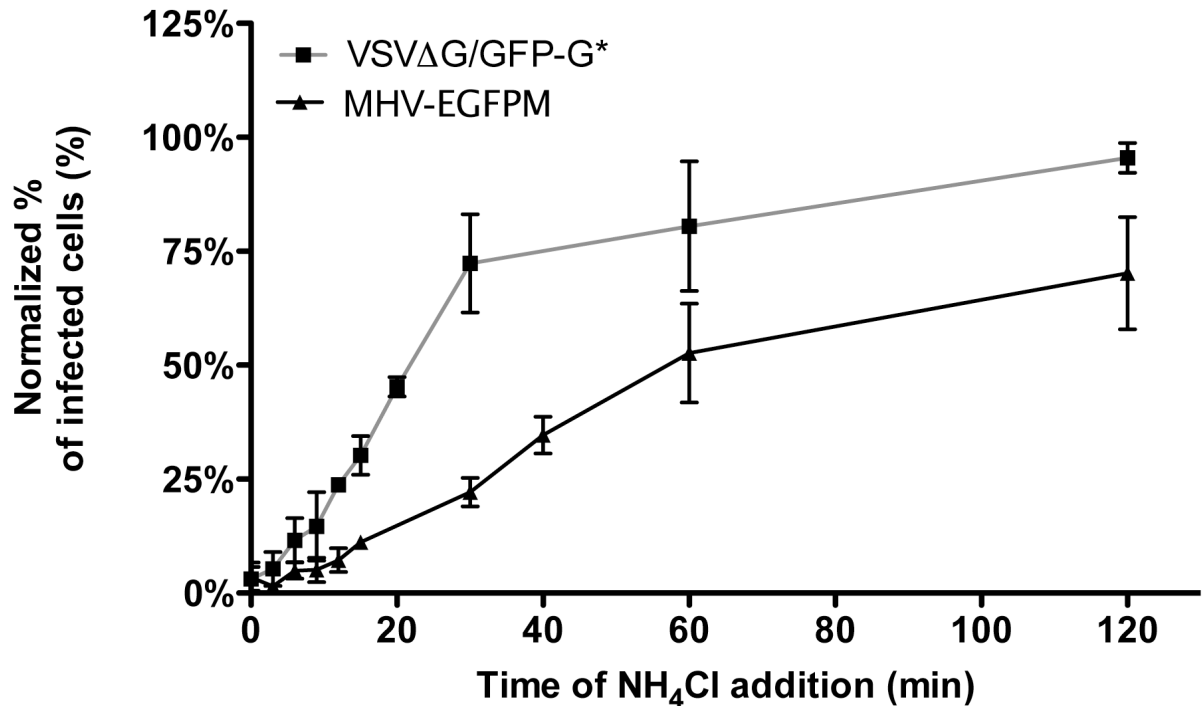
1 **Figure S2.** Effect of drug treatment on FDG uptake. (a) HEK293T cells were transfected singly  
 2 or co-transfected with plasmids encoding ΔM15 or αN. Cells were trypsinized and FDG was  
 3 added by hypotonic shock. Cells were incubated on ice for 1h and β-galactosidase activity  
 4 measured by determining the production of fluorescein using FACS. (b) HEK293T cells co-  
 5 transfected with ΔM15 and αN encoding plasmids were pretreated with the drugs used in the  
 6 fusion assay (described in 5c and f). Following pretreatment cells were trypsinized and FDG  
 7 added by hypotonic shock. Cells were incubated on ice for 1h and β-galactosidase activity  
 8 measured by determining the production of fluorescein using FACS.



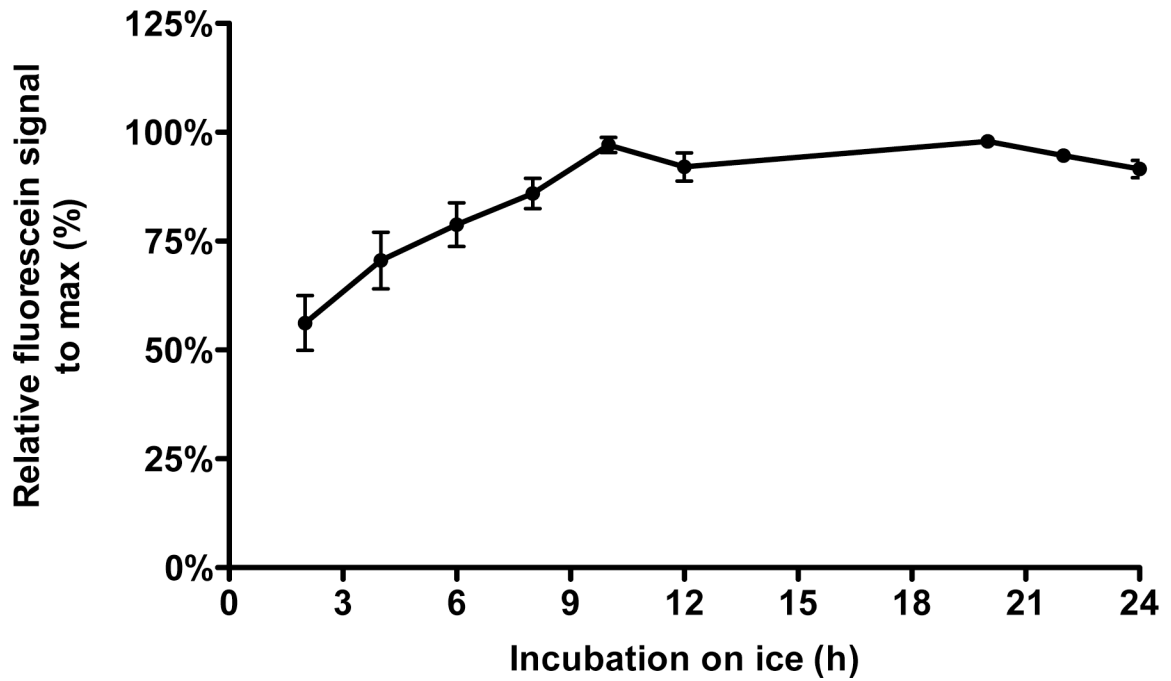
1 **Figure S3.** Growth curves of recombinant MHV- $\alpha$  viruses. Murine LR7 cells were inoculated at  
 2 MOI=1 with the recombinant and wild-type A59 strain viruses, respectively. At the indicated  
 3 times post infection, infectivity in the culture supernatants was assayed by TCID50 analysis.  
 4 Error bars represent 1 SEM, n=4.



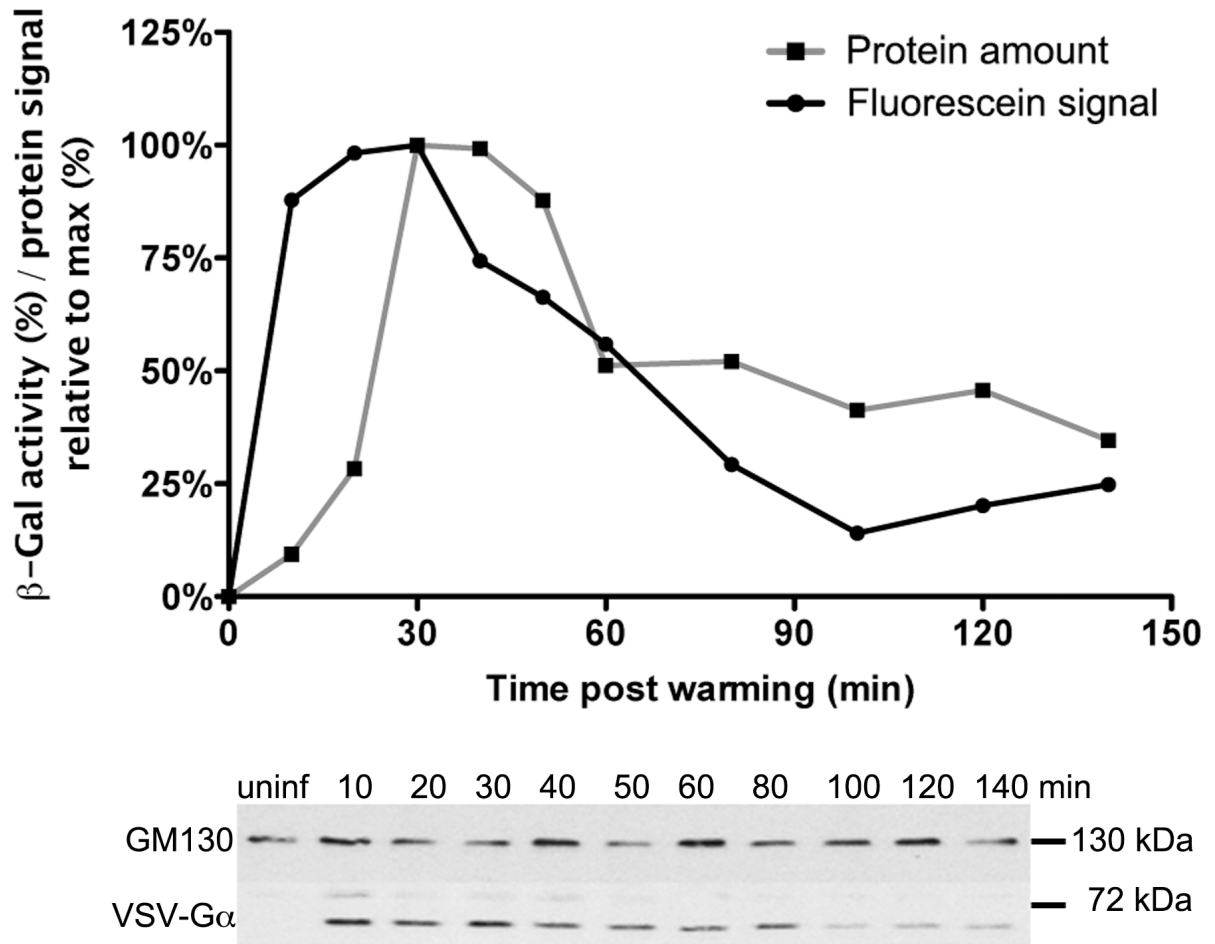
1 **Figure S4.** Morphology of negatively stained VSV $\Delta$ G/GFP-G $\alpha$  virus at neutral and low pH.  
2 20% sucrose cushion purified stocks of VSV $\Delta$ G/GFP-G $\alpha$ , resuspended in TD buffer were  
3 sequentially brought to pH 6.5 and to the final pH of 5.5. Samples were negatively stained and  
4 imaged by electron microscopy. Three representative images for pH 6.5 and pH 5.5 are shown in  
5 the left or right panel, respectively.



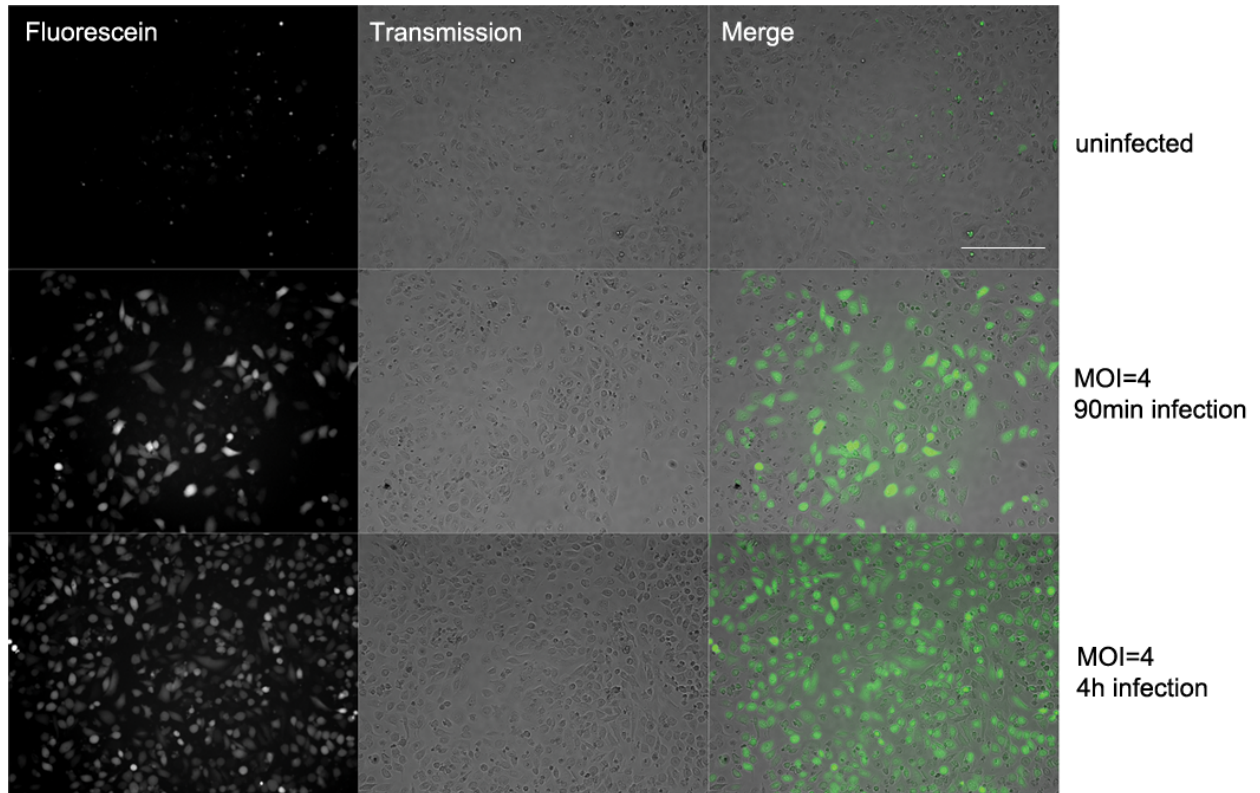
1 **Figure S5.** Virus entry kinetics of MHV and VSV as measured by their sensitivity to lysosomal  
 2 tropic agent NH<sub>4</sub>Cl. VSVΔG/GFP-G\* and MHV-EGFPM were bound to cells on ice for 90 min  
 3 at MOI=1. Unbound virus was removed with ice-cold PBS, and cultures were shifted to 37°C by  
 4 adding warm medium. NH<sub>4</sub>Cl was added at the indicated time points to stop endosome  
 5 maturation and thus virus entry. At 8h post warming, infection was scored by FACS analysis of  
 6 GFP expression. Half maximum infection of VSV was obtained within 20 min, after 40 min  
 7 approximately 80% of the maximal number of infected cells was obtained. MHV appeared to  
 8 enter cells much slower and less synchronized. After about 50 min of warming only half  
 9 maximum infection was obtained, after 100 min approximately 60% of the maximal number of  
 10 infected cells was observed. Error bars in **a** & **b** represent 1SEM, n=3.



1 **Figure S6.** Fluorescein signal dependence on the incubation on ice. LR7 $\Delta$ M15 cells were  
2 inoculated at an MOI of 10 with MHV- $\alpha$ N by binding the virus to the cells for 90 min on ice,  
3 removal of unbound virus, and shifting of the cultures to 37°C for 100min. FDG was  
4 administered by hypotonic shock and subsequently the samples were incubated on ice for the  
5 indicated amount of time.  $\beta$ -galactosidase activity was measured by determining fluorescein  
6 production using FACS.

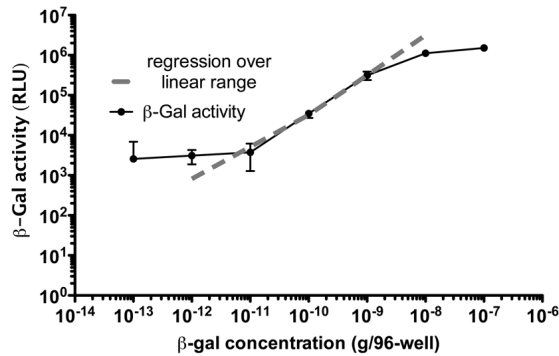


1 **Figure S7.** Intracellular  $\alpha$ -tagged protein level in relation to  $\beta$ -galactosidase activity.  
 2 VSV $\Delta$ G/Luc-G $\alpha$ \* (MOI=100) was bound to cells on ice. Unbound virus was washed off, and  
 3 culture temperature shifted to 37°C in the presence of CHX. At the indicated time points cells  
 4 were washed and trypsinized on ice. Fusion was assessed by  $\beta$ -galactosidase activity-driven  
 5 fluorescein production using FACS. In parallel samples cells were lysed and G-protein content  
 6 was measured by western blot analysis.



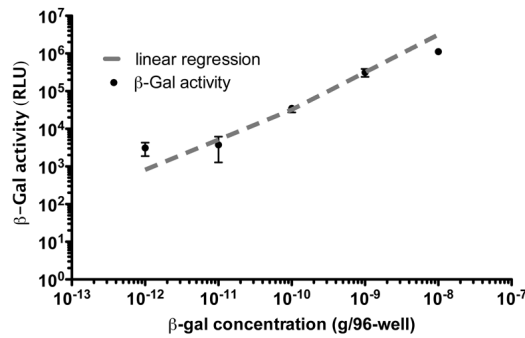
1 **Figure S8.** Fluorescence microscopy of  $\beta$ -galactosidase activity in  $\alpha$ -virus infected cells.  
2 VSV $\Delta$ G/Luc-G $\alpha^*$  virus was bound to  $\Delta$ M15 transfected HEK293T cells on ice. Unbound virus  
3 was washed off and culture temperature shifted to 37°C for the indicated time periods. Fusion-  
4 dependent  $\beta$ -galactosidase activity-driven fluorescein production in cells was visualized by wide-  
5 field fluorescence microscopy. Size bar corresponds to 250 $\mu$ m.

Using linear regression to calculate No. of Virions binding / internalizing



Calculating back from grams / well to molecules / well

Mw  $\beta$ -Galactosidase = 116519.7 (Da)  
 $N_A$  = 6.022 E23 (1/mol)  
 $Mw/N_A$  = 1.93 E-19 (g) per  $\beta$ -Galactosidase molecule



Regression over the linear range of the standard curve

$$y \text{ [RLU]} = 6.014E-5 \cdot x \text{ [\beta-Gal/well]} + 505.3$$

$$x = (y - 505.3) / 6.014E-5$$

a

b

Comparing measurement results with estimated virion numbers

Calculating the No. of active enzymes / well from RLU measurements

- Using the linear regression from the standard curve

Calculation No. of N proteins / well

No. of cells/24-well = 4.0E5

No. of N-proteins / MHV virion = 730-2200 [Ref. 31-33]

Assumption for calculations

No. N/virion = 1000

Calc. No. N/well = No. cells \* MOI \* No.N/virion

Calc. MOI = Calc No. act. enzymes / No. cells / (No. N/virion)

BINDING

MOI	$\beta$ -Gal activity (RLU)	Calc. No. of active enzymes / well	Calc. No. of N proteins / well	Calc. MOI
1	30748	5.03E+08	4.00E+08	1.26
3	76870	1.27E+09	1.20E+09	3.17
10	303005	5.03E+09	4.00E+09	12.57

c

INTERNALIZATION

MOI	$\beta$ -Gal activity (RLU)	Calc. No. of active enzymes / well	Calc. No. of N proteins / well	Calc. MOI
10	33004	5.40E+08	4.00E+09	1.35
30	82510	1.36E+09	1.20E+10	3.41
100	243213	4.04E+09	4.00E+10	10.09

d

1 **Figure S9.** Calculating virus binding and internalization using a standard curve. (a) Correlation  
 2 between  $\beta$ -galactosidase activity and amount of  $\beta$ -galactosidase protein with indicated linear  
 3 range. Increasing amounts of purified wild-type *E. coli*  $\beta$ -galactosidase were added to cell lysates  
 4 of LR7 $\Delta$ M15 cells. Samples were probed with Beta-Glo<sup>®</sup> substrate and incubated for 40 min at  
 5 RT in the dark before measuring the  $\beta$ -galactosidase activity using a luminescence read-out. (b)  
 6 Linear range of the  $\beta$ -galactosidase activity of the standard curve. (c) Calculation of number of  
 7 active enzymes per well from the standard curve and correlation thereof with the estimated  
 8 number of N proteins present in the binding assay based on literature.[1-3] (d) Calculation of the  
 9 number of active enzymes per well from the standard curve and correlation thereof with the  
 10 estimated number N proteins per well in the internalization assay.

## REFERENCES

1. Beniac DR, Andonov A, Grudeski E, Booth TF (2006) Architecture of the SARS coronavirus prefusion spike. *Nature structural & molecular biology* 13: 751-752.
2. Escors D, Camafeita E, Ortego J, Laude H, Enjuanes L (2001) Organization of two transmissible gastroenteritis coronavirus membrane protein topologies within the virion and core. *Journal of virology* 75: 12228-12240.
3. Neuman BW, Kiss G, Kunding AH, Bhella D, Baksh MF, et al. (2011) A structural analysis of M protein in coronavirus assembly and morphology. *Journal of structural biology* 174: 11-22.